HEALTH AND MEDICINE

Synthetic "smart gel" provides glucose-responsive insulin delivery in diabetic mice

Akira Matsumoto,[1]*† Miyako Tanaka,[2]* Hiroko Matsumoto,[1] Kozue Ochi,[2] Yuki Moro-oka,[1] Hirohito Kuwata,[2,3] Hironori Yamada,[1] Ibuki Shirakawa,[4] Taiki Miyazawa,[1] Hitoshi Ishii,[3] Kazunori Kataoka,[5,6] Yoshihiro Ogawa,[7,8,9] Yuji Miyahara,[1] Takayoshi Suganami[2]†

Although previous studies have attempted to create "electronics-free" insulin delivery systems using glucose oxidase and sugar-binding lectins as a glucose-sensing mechanism, no successful clinical translation has hitherto been made. These protein-based materials are intolerant of long-term use and storage because of their denaturing and/or cytotoxic properties. We provide a solution by designing a protein-free and totally synthetic material–based approach. Capitalizing on the sugar-responsive properties of boronic acid, we have established a synthetic polymer gel–based insulin delivery device confined within a single catheter, which exhibits an artificial pancreas–like function in vivo. Subcutaneous implantation of the device in healthy and diabetic mice establishes a closed-loop system composed of "continuous glucose sensing" and "skin layer"–regulated insulin release. As a result, glucose metabolism was controlled in response to interstitial glucose fluctuation under both insulin-deficient and insulin-resistant conditions with at least 3-week durability. Our "smart gel" technology could offer a user-friendly and remarkably economic (disposable) alternative to the current state of the art, thereby facilitating availability of effective insulin treatment not only to diabetic patients in developing countries but also to those patients who otherwise may not be strongly motivated, such as the elderly, infants, and patients in need of nursing care.

INTRODUCTION

Diabetes is a major global health threat that poses a devastating impact on society (*1*, *2*). Among a growing lineup of medications for diabetes, insulin therapy continues to be a primary option in clinical practice for both palliative and preventive purposes (*3*). A number of studies have shown that tight glycemic control achieved with intensive insulin regimes can effectively reduce the risk of developing or escalating complications (*1*, *4*–*6*). Currently, the most common modality of this treatment is the patients' self-administration, termed "open-loop" insulin delivery. However, this method inevitably suffers from inaccuracy of the dose control, where the overdose must be strictly avoided, otherwise causing acute and fatal hypoglycemia. Recently, a growing effort has been focused on the development of a "closed-loop" or a self-regulated type of insulin delivery system that is able to continuously deliver more accurate amount of insulin in response to the change in blood glucose concentrations. These so-called "artificial pancreas" systems typically combine subcutaneously implanted glucose sensors and automated algorithm-driven insulin infusing modules that are either electrically or wirelessly communicable (*3*, *7*, *8*). Although accumulating reports validate this approach, limitations also persist. As for "electronics-derived" issues, the need for frequent calibration and maintenance may impair ease of use and thus the users' quality of life (QOL). In addition, these technologies may raise the cost of diabetes therapy.

Accordingly, there are also constant research efforts focusing on "electronics-free" approaches to the development of artificial pancreas systems (*9*–*13*). The use of glucose oxidase (GOD) and a sugar-binding lectin, Concanavalin A (Con A), are two representative strategies often harnessed to endow the homing polymeric materials with the prerequisite glucose sensitivities (*9*–*12*, *14*, *15*). However, these protein-based materials are not amenable to long-term use and storage because of their denaturing and cytotoxic properties. As a consequence, to our knowledge, no successful clinical translation of these systems has hitherto been made.

To overcome those limitations, a protein-free and thoroughly synthetic material–based approach is worth exploring. Phenylboronic acid (PBA) derivatives readily complex with 1,2- and 1,3-*cis*-diols, including those found in carbohydrates, through reversible boronate ester formation in an aqueous solution (*16*–*21*). Their binding strength and specificity can be widely tailored on the basis of stereochemistry and controlled electronic effect. This unique chemistry has already borne fruit as the molecular bases for synthetic glucose sensors, bioseparations, and other diagnostic and therapeutic applications (*22*–*24*). A recent work by Anderson *et al.* (*25*) has described a new type of "smart" long-lasting insulin that is responsive to glucose based on this creative PBA-involved engineering. Our previous in vitro studies had demonstrated the following:

1. A glucose-dependent shift in the equilibria of PBA (between uncharged and anionically charged; Fig. 1A), when integrated with optimally amphiphilic acrylamide gel backbone (Fig. 1B), could induce a reversible, glucose-dependent change in hydration of the gel (*16*).

2. The resultant abrupt and rapid change in hydration, under optimized conditions, led to the formation of a gel surface–emerging, microscopically dehydrated layer, so-called "skin layer", providing a mode that is able to effectively switch the release (diffusion) of the gel-loaded insulin (Fig. 1C) (*19*).

[1]Institute of Biomaterials and Bioengineering, Tokyo Medical and Dental University, Tokyo, Japan. [2]Department of Molecular Medicine and Metabolism, Research Institute of Environmental Medicine, Nagoya University, Nagoya, Japan. [3]Department of Diabetology, Nara Medical University, Nara, Japan. [4]Department of Organ Network and Metabolism, Graduate School of Medical and Dental Sciences, Tokyo Medical and Dental University, Tokyo, Japan. [5]Innovation Center of NanoMedicine, Kawasaki Institute of Industrial Promotion, Kawasaki, Japan. [6]Policy Alternatives Research Institute, University of Tokyo, Tokyo, Japan. [7]Department of Molecular Endocrinology and Metabolism, Graduate School of Medical and Dental Sciences, Tokyo Medical and Dental University, Tokyo, Japan. [8]Department of Medicine and Bioregulatory Science, Graduate School of Medical Sciences, Kyushu University, Fukuoka, Japan. [9]Japan Agency for Medical Research and Development, Core Research for Evolutional Science and Technology (CREST), Tokyo, Japan.
*These authors contributed equally to this work.
†Corresponding author. Email: matsumoto.bsr@tmd.ac.jp (A.M.); suganami@riem.nagoya-u.ac.jp (T.S.)

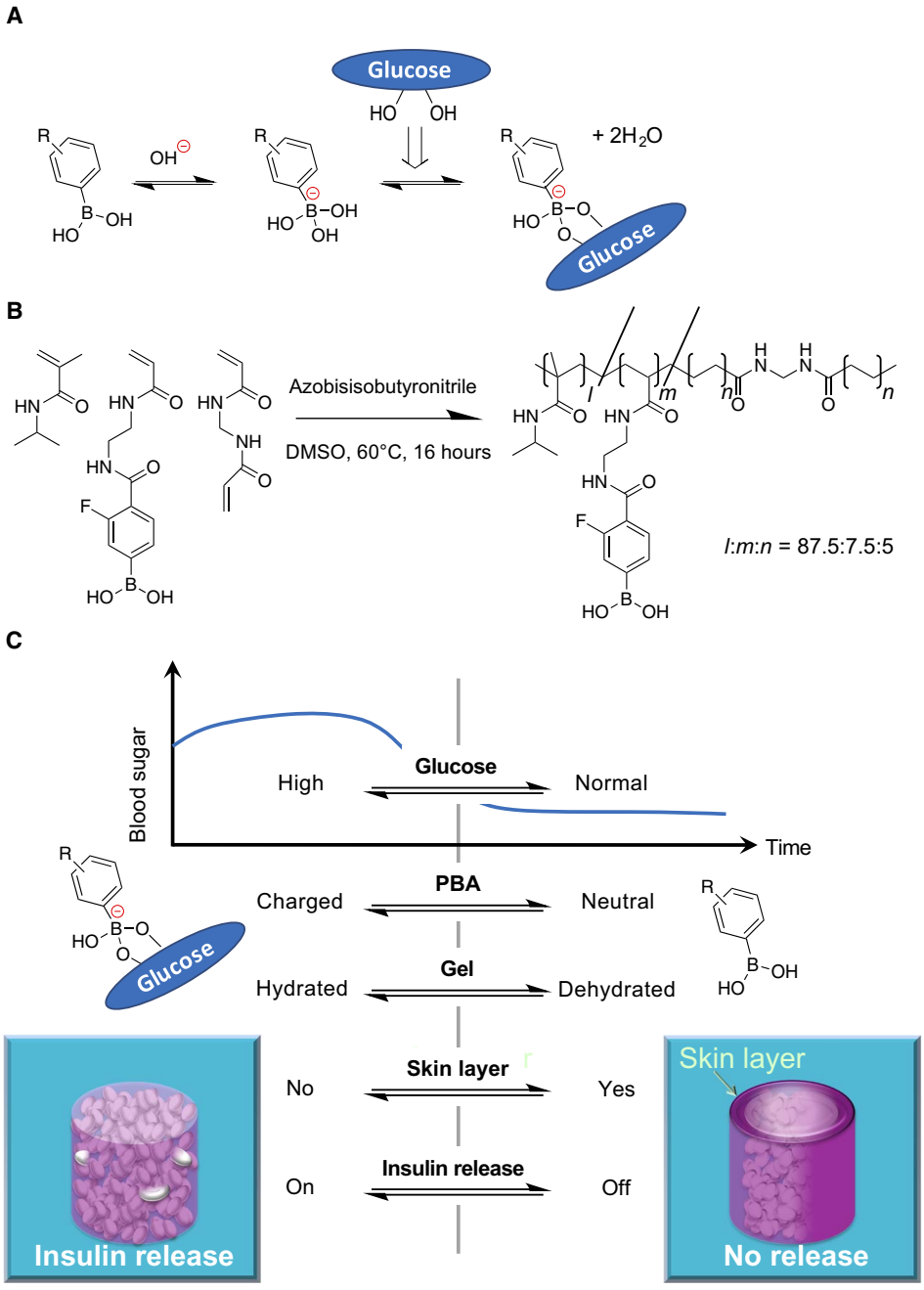

Fig. 1. Structure and principle of the boronate gel–based insulin delivery system. (**A**) Glucose-dependent equilibria of PBA derivatives. (**B**) Chemical structure of glucose-responsive gel. Monomers and their polymerized (cross-linked) chemical structures are shown with their optimized molar fraction (*l*:*m*:*n* = 87.5:7.5:5) to yield the glucose sensitivity under physiological conditions (pH 7.4 and 37°C) accompanied by a threshold concentration of glucose at normoglycemic (100 mg/dl) (above which the gel delivers insulin). DMSO, dimethyl sulfoxide. (**C**) Schematic illustration of "pancreas-like" self-regulated insulin delivery function of the gel.

3. The chemical structure of the gel could be further optimized so that it undergoes the above-mentioned performance under physiologically relevant conditions, accompanied by a remarkably "gated" manner in response to the level of normoglycemia (*17*, *18*, *20*, *21*).

However, this approach using PBA gel is yet to be validated in vivo.

Here, we describe a catheter-combined device that is suitably scaled for mouse model experiments and demonstrate that it can serve as an "electronics-free" and "totally synthetic" artificial pancreas with feasible safety, efficacy, and durability. This remarkably simple, diffusion-based principle may offer a number of advantages over the above-mentioned algorithm-controlled or enzymatically driven systems in terms of cost, stability, and ease of manufacturing, transport, storage, and maintenance, offering a more robust and easy-to-prevail (even to developing regions of the world) type of platform technology. In addition, advantageously, the pre-gel solution, which instantly gels upon heating, can

fill virtually any desired shape and dimension and therefore can be combined with other well-established medical device technologies such as (micro)needles, catheters, and many other implantable forms.

RESULTS

Characterization of glucose-responsive gel

Figure 2A provides images of the gel formed in a macroscopic slab shape that is equilibrated under different glucose environments, that is, hyperglycemic (1000 mg/dl; left) and no glucose (right) conditions. As mentioned above, the chemical structure of this gel has been designed (Fig. 1B) so as to evoke a glucose-dependent change in hydration with a threshold value (of glucose concentration) exactly at normoglycemia (100 mg/dl) under physiological aqueous conditions (pH 7.4; 37°C; 155 mM NaCl; fig. S1) (*18*). Apparently, different sizes of the gel between the two states indicate correspondingly different levels of the hydration. One can also appreciate that the gel retains its opaque (light-scattered) color on its surface when equilibrated without glucose (Fig. 2A, right) due to the occurrence of the skin layer, a surface-localized microscopic dehydration, which recovers into a more hydrated and transparent state when equilibrated under hyperglycemic condition (Fig. 2A, left) (see also fig. S2).

Figure 2B depicts a typical result of a insulin release experiment using the gel when challenged by preprogrammed patterns of glucose using a high-performance liquid chromatography (HPLC) setup (see Materials and Methods). For this experiment and the following in vitro study, a cylindrically shaped "capillary" gel (50 mm long and 1 mm in diameter) was used (see Materials and Methods). It is demonstrated in Fig. 2B that the release of insulin from the gel (bottom) is continuously controllable by the role of the skin layer with close correspondence to the pattern of glucose (top). Note that the observed fluorescence intensity in Fig. 2B (bottom) does not linearly correlate with the concentration of insulin in the milieu; in the equilibrium state, the rate of insulin release observed at the glucose concentrations of 200 mg/dl or higher was found to be at least two orders of magnitude greater than that observed under normoglycemic (100 mg/dl) conditions, in accordance with our previous report (see also Materials and Methods) (*18*).

Figure 2 (C to E) demonstrates in vitro validation of the gel in terms of its capability for glucose-dependent release of insulin and its inert effect on insulin bioactivity. Namely, the gel pieces were exposed to insulin-sensitive (differentiated 3T3-L1) adipocytes in the culture medium containing different concentrations of glucose, that is, 450 and 100 mg/dl, glucose values mimicking hyperglycemic and normoglycemic conditions, respectively (Fig. 2C). As a control, 1 nM Humulin R was administered in the culture. The glucose concentrations were monitored for up to 24 hours. Here, insulin-dependent and insulin-independent glucose uptake gave rise to a decrease in glucose concentrations of the medium. The amount of insulin-independent glucose uptake was calculated using the culture with adipocytes alone. Thus, the data on the insulin-dependent glucose uptake are shown in Fig. 2D. Under high-glucose conditions, the amount of insulin-dependent glucose uptake was almost comparable between experimental and control cultures (Fig. 2D, left). In contrast, glucose uptake was negligible in the culture with "insulin gel" under the low-glucose conditions, as compared to the Humulin-treated control (Fig. 2D, right). These results are presumably due to the role of the skin layer, which effectively blocks the release of insulin under normoglycemic conditions. The amount of cumulative insulin release in the culture continuously increased under the high-glucose conditions throughout the experimental period, whereas that under low-glucose conditions was stable (Fig. 2E). Collectively, these observations support the capability of the gel to serve an artificial pancreas–like function, that is, glucose-dependent release of insulin in vitro, as illustrated in Fig. 1C, along with its inert effect on the activity of insulin.

Catheter-combined device

The fabrication procedure for the catheter-combined device is summarized in Fig. 3 with some key micro- and macroscopic overviews. Briefly, 4-French (1.2 mm of diameter) silicone catheters bearing number-, size-, and pitch-controlled penetrating pores perpendicular to the long axis were prepared by optimized three-dimensional (3D) laser irradiation technique (Fig. 3, A and B). Before gelation, the catheter surface was treated with a silane coupling agent bearing methacrylate functionality to warrant the stability in the following gel attachment. The molded gelation (Fig. 3C) was then carried out in a way that the gel occupies the whole inner wall of the catheter and the openings, as indicated in Fig. 3E. The outermost surface of the device was further coated with a thin layer of poly(ethyleneglycol) to reduce unwanted biofouling upon subcutaneous implantation and also to reinforce the overall mechanical integrity (figs. S3 to S7). The gel-modified catheter was then cut into 15-mm-long pieces, and each of them was connected with another longer (11 cm) piece of nontreated catheter (Fig. 3F); the thus-installed "long-tail" part served as an insulin reservoir. Figure 4A illustrates an operating principle of the device to achieve an artificial pancreas–like function via skin layer–driven diffusion control of insulin, the rate of which is readily scalable by tuning the number of the openings on the wall. Figure 4B shows a representative result of insulin release from the device, revealing a good synchronization between the pattern of glucose (top) and the insulin release (bottom), similar to Fig. 2B.

It is important to address the biosafety of the device. In vitro experiments were performed using Chinese hamster lung fibroblasts (V79). Conditioned medium prepared from the culture of the device in M05 medium did not affect colony formation of V79 cells, suggesting no detectable cytotoxicity of the device after autoclaving (fig. S8A). Moreover, we implanted the device under the skin of normoglycemic mice for a week to investigate the biosafety in vivo (fig. S8, B to E). The mice were divided into two groups: mice implanted with the control silicone catheter and the catheter-combined device. There was no significant difference in the population of circulating immune cells and mRNA expression of the genes related to inflammation between the groups (fig. S8, B and C). Histological examinations revealed that mild inflammatory cell infiltration and fibrotic changes occurred around the device to a similar extent, as observed around the clinically available silicone catheter (fig. S8, D and E). These observations suggest that the device meets the clinically required biosafety.

Evaluation of glucose-responsive insulin release in vivo

We then examined how this insulin delivery device works in response to acute nutritional changes such as starvation and hyperglycemia in healthy mice (Fig. 5A, top). Although there was a slight decrease in blood glucose concentrations in mice implanted with the device containing recombinant human insulin (Humulin R), it was not severe hypoglycemia (Fig. 5A, GTT-1). The glucose tolerance test revealed that the human insulin–loaded device markedly suppressed a transient increase in blood glucose concentrations compared to the PBS-loaded device. Notably, the glucose-lowering effect was observed as early as 15 min after the glucose injection. Moreover, the device was still effective 7 days after the initial experiment, indicating the durability and stability necessary for future clinical use (Fig. 5A, GTT-2). In parallel, we

confirmed that serum concentrations of human insulin were markedly increased by acute glucose injection and then decreased at 60 min (Fig. 5A, GTT-1 and GTT-2), directly supporting the on-off function of the device depending on circumferential glucose levels. Under these experimental conditions, the serum concentrations of mouse C-peptide were significantly decreased in the human insulin–treated mice relative to the control mice (Fig. 5A, GTT-2). There was no apparent reduction of loaded insulin levels in the device after a series of glucose tolerance tests. Moreover, the device was therapeutically effective for at least 3 weeks in mice (fig. S9, A and B). Notably, under ad lib–fed conditions, only baseline

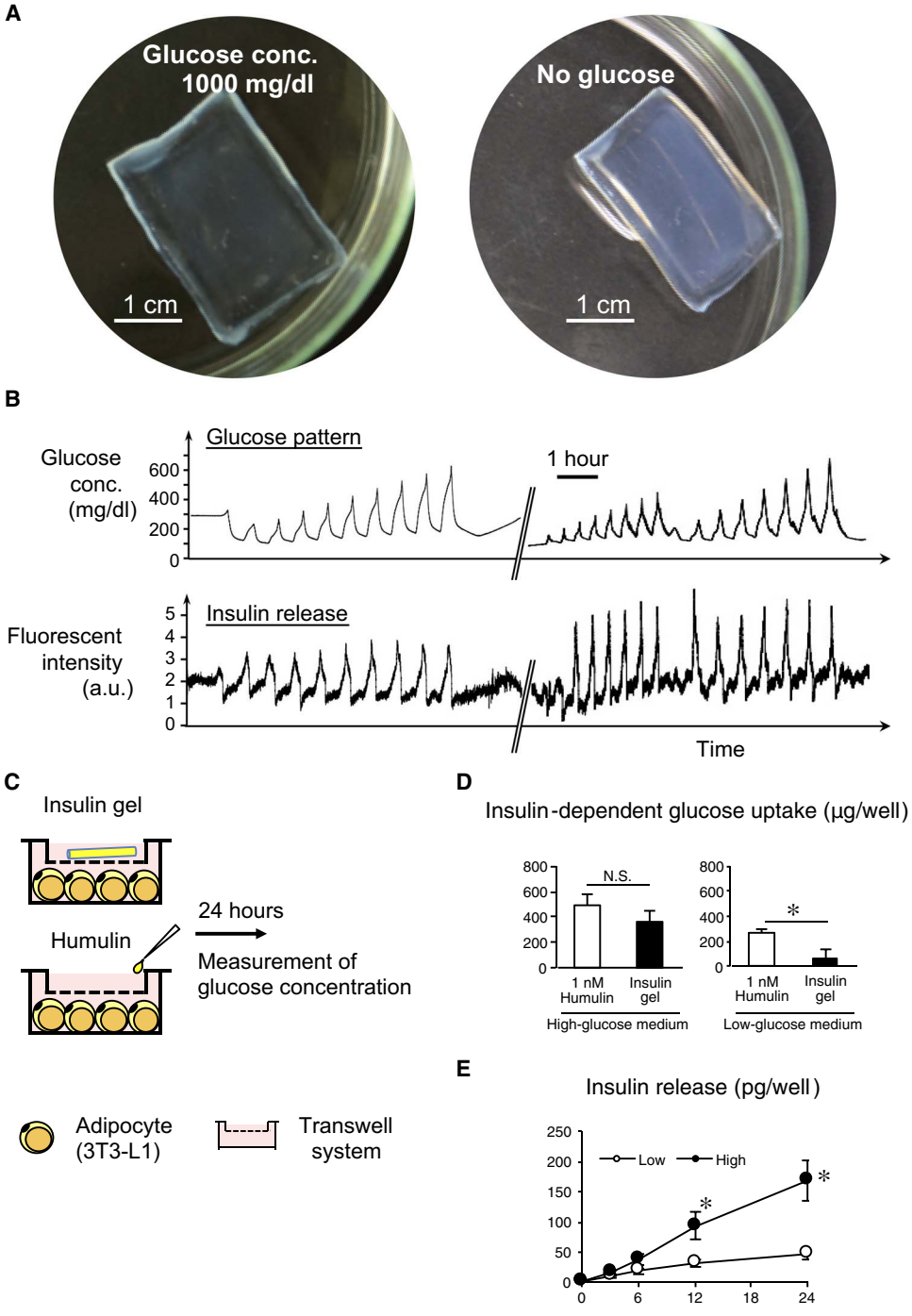

Fig. 2. Characterization of the glucose-responsive gel in vitro. (**A**) Images of a smart gel formed in a macroscopic slab shape equilibrated under hyperglycemic (1000 mg/dl) (left) and no-glucose (right) conditions. (**B**) Release experiment. Top: Temporal patterns of glucose fluctuation challenged through a HPLC setup under physiological conditions (pH 7.4; 37°C; 155 mM NaCl). Bottom: Time course change in fluorescence intensity of fluorescein isothiocyanate (FITC)–labeled bovine insulin released from the gel. The break in the *x* axis indicates an overnight interval between two experiments during which the gel was kept under constant flow (1 ml/min) of phosphate-buffered saline (PBS) containing glucose (100 mg/dl). a.u., arbitrary units. (**C**) Protocol for in vitro glucose-uptake assessment using differentiated 3T3-L1 adipocytes. (**D**) Insulin-dependent glucose uptake by the adipocytes. N.S., not significant. (**E**) Amount of cumulative insulin release in the culture. $^*P < 0.05$. $n = 4$.

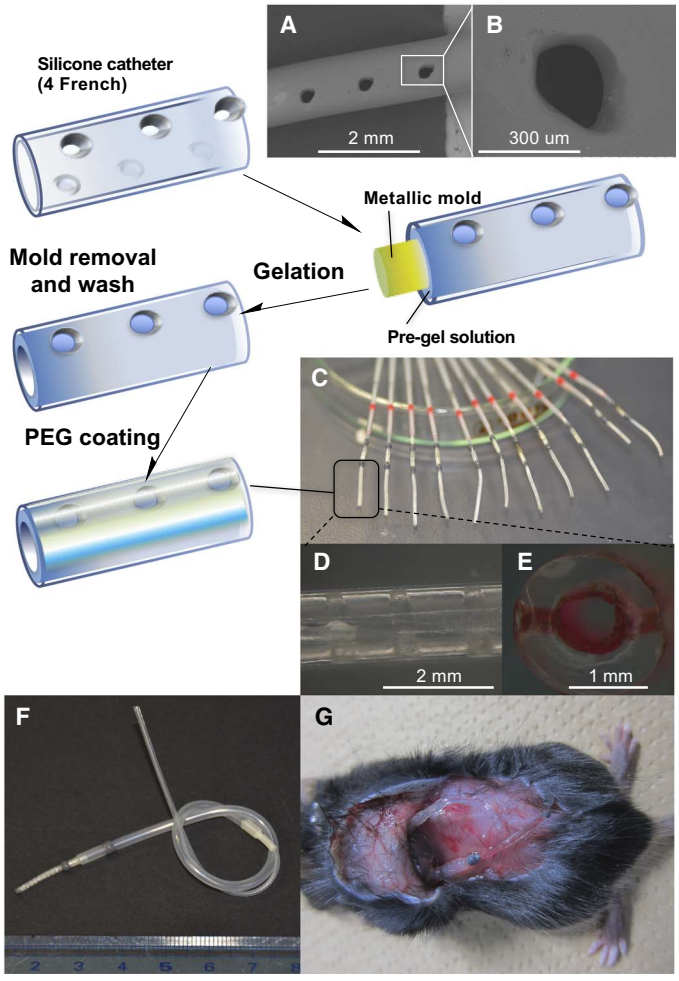

Fig. 3. Fabrication of catheter-combined device. (**A** and **B**) SEM images of 4-French (1.2 mm in diameter) silicone catheter bearing penetrating (perpendicular to the long axis) openings on the wall made by laser irradiation. (**C** to **E**) Overview (C), side view (D), and cross-sectional transmittance images (E) of the gel-modified catheter (the gel was stained by red-colored ink). (**F** and **G**) Overview of the ready-to-use device installed with the upstream (long tail) reservoir filled with insulin and its appearance on subcutaneous implantation. PEG, poly(ethyleneglycol).

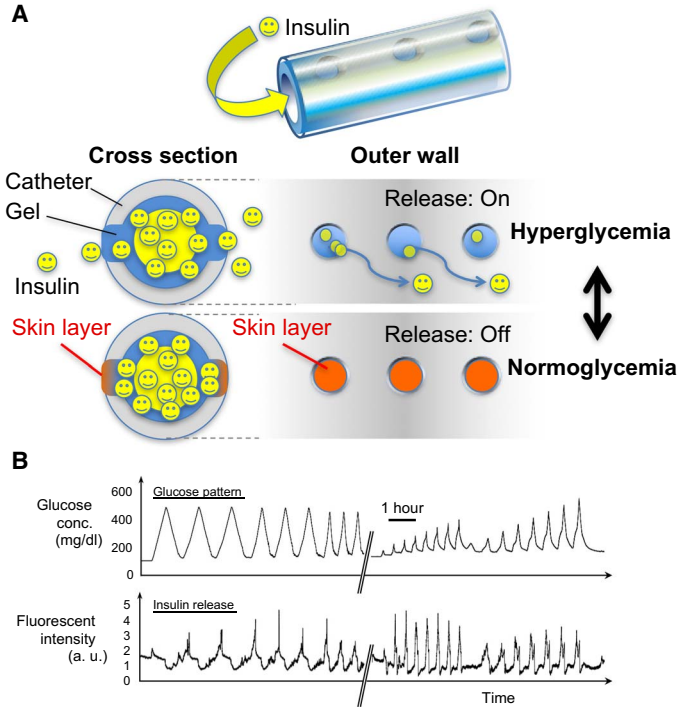

Fig. 4. Working principle and behavior of catheter-combined device. (**A**) Schematic illustration of skin layer–driven glucose-dependent diffusion control of insulin accomplished by the catheter-combined device. (**B**) Release experiment under physiological conditions using a HPLC setup. Top: Temporal patterns of glucose. Bottom: Time course change in fluorescence intensity of FITC-labeled bovine insulin released from the gel. The break in the *x* axis indicates an overnight interval between two experiments during which the device was kept under constant flow (1 ml/min) of PBS containing glucose (100 mg/dl).

levels of insulin release from the device were observed in the human insulin–treated mice, whose blood glucose concentrations were almost comparable to those in the control mice (fig. S9, B and C). These observations indicate that our insulin delivery device is capable of a rapid response to the glucose concentrations in the subcutaneous interstitium surrounding the device, thereby mitigating endogenous insulin secretion from pancreatic β cells.

We next injected different doses of glucose into the mice to gain insight into the conditions under which the device can respond to the interstitial glucose concentrations surrounding the device (Fig. 5B). Here, the recombinant human insulin–loaded device effectively lowered the blood glucose concentrations in mice receiving the higher doses (2 and 3 g/kg body weight) of glucose, whereas only a marginal effect was observed in those receiving 1 g/kg body weight of glucose. We further examined the effects of other sweeteners, such as monosaccharide fructose and artificial sweetener aspartame, on the device (Fig. 5C). Administration of the physiological amount of fructose (corresponding to the amount included in eight oranges) and aspartame (corresponding to the daily consumption limit recommended by World Health Organization) did not show a substantial effect on blood glucose concentrations in the mice implanted with the recombinant human insulin– and PBS-loaded devices. Thus, these observations support dose-dependent dynamics and glucose-specific behavior of the device and consequently led us to assess the therapeutic efficacy for diabetes in mice.

Therapeutic efficacy for diabetes in mice

We then examined the effect of the device on glucose metabolism in streptozotocin (STZ)–induced type 1 diabetes (conditions with absolute insulin deficiency) in mice (Fig. 6A). Seven days after implantation of the recombinant human insulin–loaded device, there was a marked reduction in ad lib blood glucose concentrations along with the amount of water intake in type 1 diabetic mice (Fig. 6B). In line with this, the otherwise reduced body weight and epididymal fat weight were significantly increased in the recombinant human insulin–treated type 1 diabetic mice (Fig. 6B). In the glucose tolerance test, the treatment roughly normalized the basal blood glucose concentrations after overnight fasting and effectively ameliorated the glucose intolerance (Fig. 6C). Notably, the serum human insulin concentrations increased in response to the acute glucose injection even under diabetic conditions (Fig. 6C), suggesting that our device is capable of controlling glucose fluctuation and mean blood glucose concentrations. We confirmed that the treatment restored the dysregulated mRNA expression of the genes related to glucose and lipid metabolism in type 1 diabetic mice (Fig. 6D).

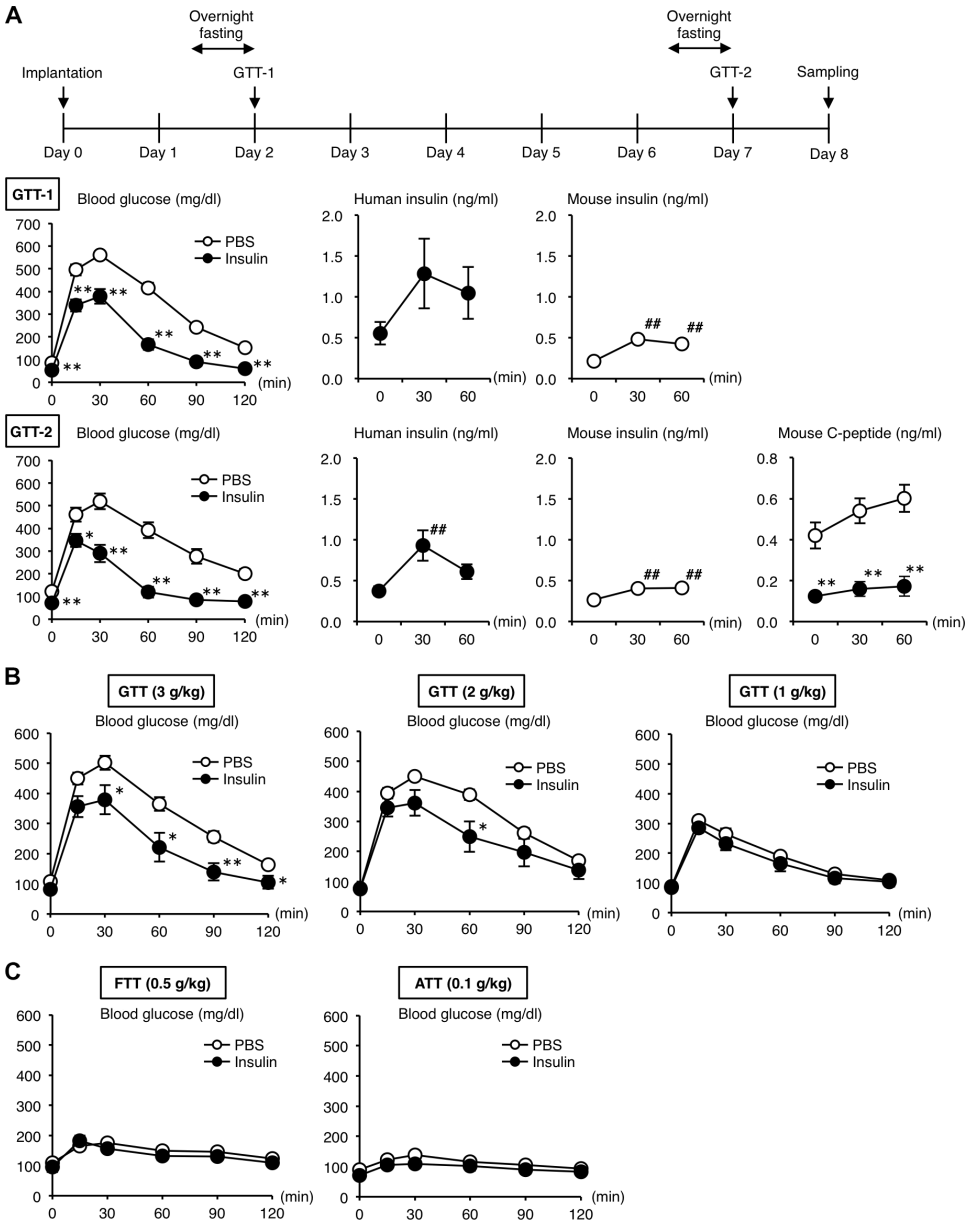

Fig. 5. Evaluation of glucose-responsive insulin release in vivo. (**A**) Protocol of the experimental design using healthy mice. (**B**) Glucose tolerance test (GTT). Glucose (3 g/kg body weight) was injected intraperitoneally 2 and 7 days after the implantation of the devices. $^{**}P < 0.01$ and $^{*}P < 0.05$ versus PBS group. $^{\#\#}P < 0.01$ and $^{\#}P < 0.05$ versus 0 min. $n = 8$ to 12. (B) GTT with different dosage of glucose (1, 2, and 3 g/kg body weight). $^{*}P < 0.05$. $n = 10$. (**C**) The fructose tolerance test (FTT) (fructose, 0.5 g/kg body weight) and the aspartame tolerance test (ATT) (aspartame, 0.1 g/kg body weight). $^{**}P < 0.01$ and $^{*}P < 0.05$. $n = 8$.

The device significantly lowered the blood glucose concentrations at ad lib at day 1 after implantation (Fig. 6E). Moreover, we monitored hemoglobin A1c (HbA1c) levels and found that the treatment effectively reversed the otherwise increased HbA1c levels in type 1 diabetic mice (Fig. 6F).

We next examined the therapeutic efficacy of the device using diet-induced obese mice, since most of the patients belong to type 2 diabetes (conditions with insulin resistance or relative insulin deficiency). After 4 weeks of high-fat diet feeding when the mice developed hyperinsulinemic insulin-resistant type 2 diabetic conditions, they were implanted with the recombinant human insulin– or PBS-loaded devices and then were subjected to the glucose tolerance test (Fig. 7, A to C). The recombinant human insulin–loaded device effectively ameliorated the high-fat diet–induced glucose intolerance (Fig. 7C). There was also a slight but significant decrease in blood glucose concentrations in mice implanted with the recombinant human insulin–loaded device compared to those implanted with the PBS-loaded device (Fig. 7C). Here, the treatment significantly lowered the otherwise elevated serum mouse C-peptide concentrations in high-fat diet–fed mice (Fig. 7C), suggesting that the device effectively mitigates obesity-induced hyperinsulinemia. Notably, the treatment did not affect the body weight and tissue weights of epididymal fat and liver in obese mice (Fig. 7D), although it is known that hyperinsulinemia sometimes increases body weight and adiposity, thereby inducing further insulin resistance. Together, these observations

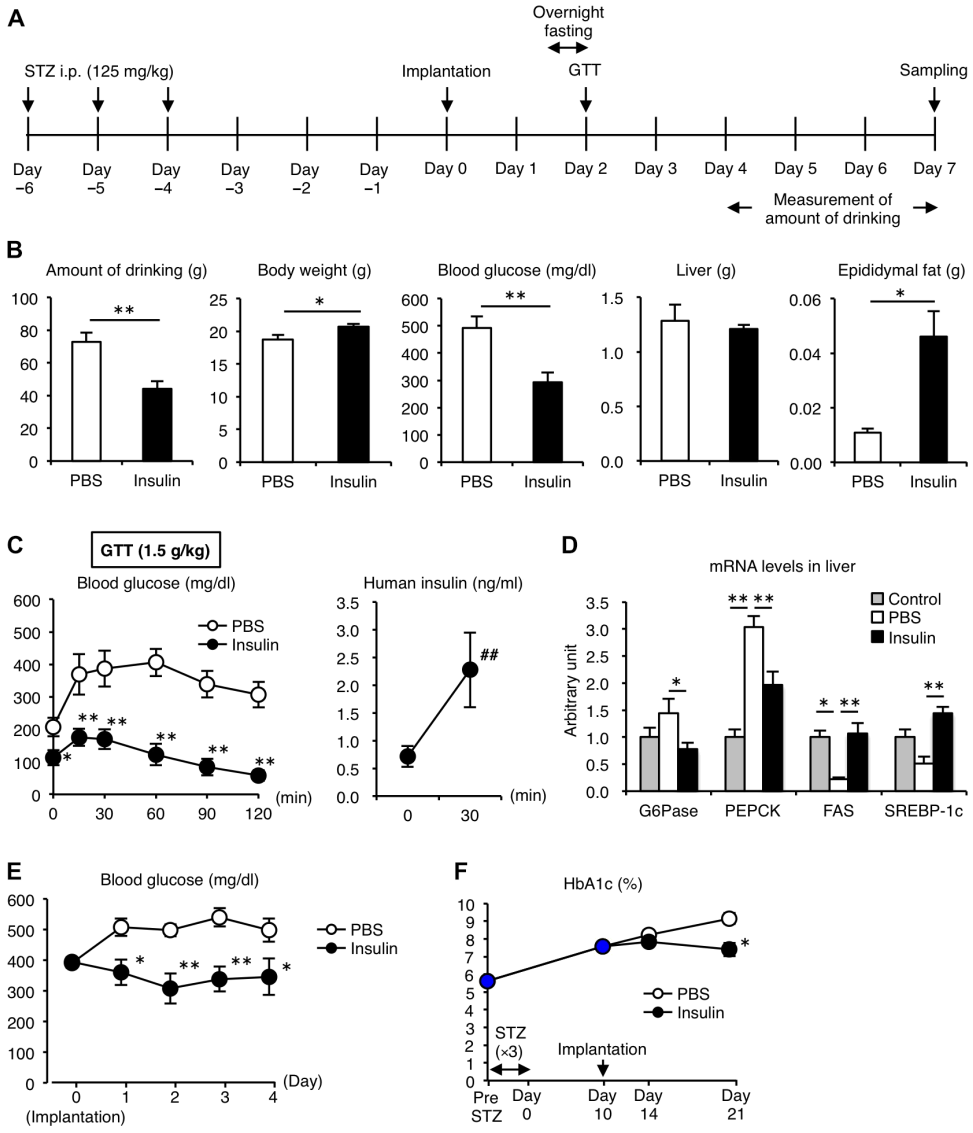

Fig. 6. Therapeutic efficacy for type 1 diabetes in mice. (**A**) Protocol of the experimental design. Type 1 diabetic models were induced by the intraperitoneal (i.p.) injection of STZ (125 mg/kg body weight) for 3 consecutive days. (**B**) Amount of drinking during the last 3 days of the experimental period and body weight, blood glucose concentrations, and tissue weights of the liver and epididymal fat at day 7. (**C**) Blood glucose concentrations and serum human insulin concentrations in the GTT (glucose, 1.5 g/kg body weight). (**D**) mRNA expression of glucose-6-phosphatase (G6Pase), phosphoenolpyruvate carboxykinase (PEPCK), fatty acid synthase (FAS), and sterol regulatory element–binding protein-1c (SREBP-1c) in the liver. $^{**}P < 0.01$ and $^{*}P < 0.05$ versus PBS group. $^{\#\#}P < 0.01$ versus 0 min. $n = 6$ to 12. (**E**) Blood glucose concentrations under ad lib–fed conditions after implantation of the device. $^{*}P < 0.05$. $n = 6$ to 12. (**F**) Time course of HbA1c. Type 1 diabetic mice were implanted with the device containing PBS and human insulin. $^{*}P < 0.05$. $n = 4$.

indicate that our insulin delivery device is capable of controlling glucose metabolism under both insulin-deficient and insulin-resistant conditions and firmly establish the safety and efficacy of our electronics-free and totally synthetic material–based approach.

DISCUSSION

Here, we demonstrate that our smart gel and catheter-combined simple device scaled suitable for mouse model experiment can provide an artificial pancreas–like function with the feasible safety and efficacy, for the first time, on totally synthetic materials and electronics-free bases. In all ongoing closed-loop approaches, insulin pharmacokinetics, which matters because of a gap between interstitial and intravascular glucose concentrations resulting in certain lag time in the glucose-lowering action, is a central challenge, and therefore, much effort has been focused on improvement of the controlling algorithm (*3*, *8*). The beauty of the "skin layer" rationale described here may lie in the fact that it is a gel surface–localized (within at most a few hundred micrometers in thickness) dynamic event, which enables a markedly rapid on-off switching behavior (*19*). It also enables a long-term sustained and repeatable pattern of response; that is, the pattern of insulin release does not change essentially for days. These features cannot be easily realized through ongoing research efforts that capitalize on nanoparticle formulation techniques (*11*, *12*); those approaches inevitably result in a burst-like

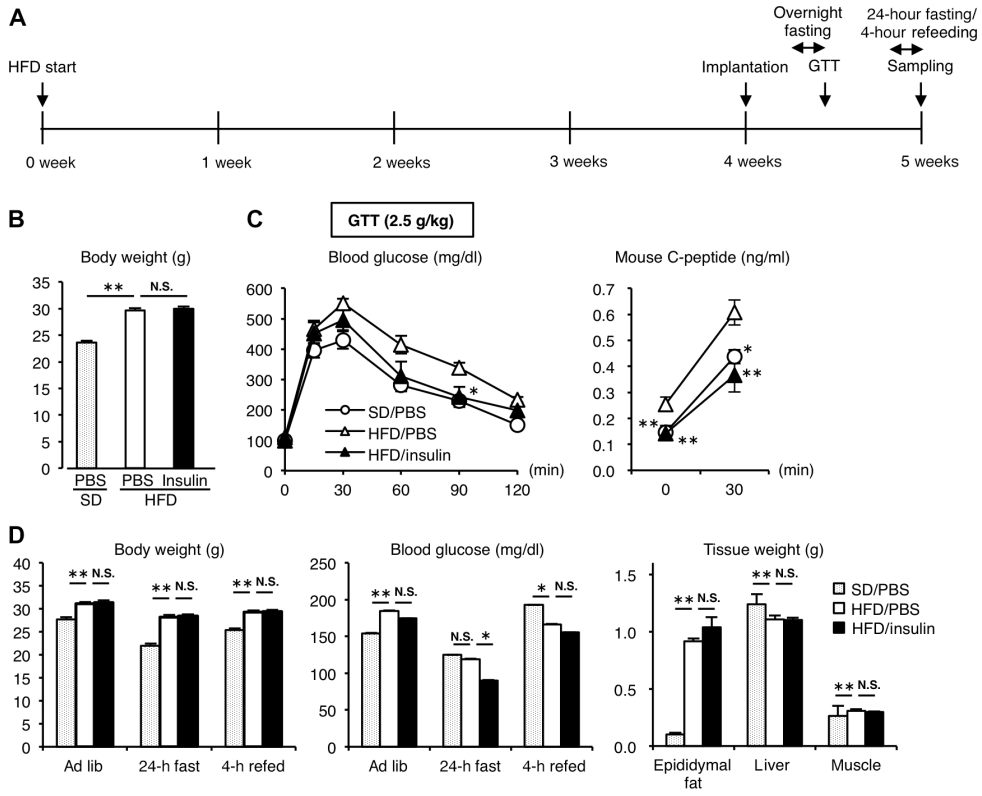

Fig. 7. Therapeutic efficacy for type 2 diabetes in mice. (**A**) Protocol of the experimental design. HFD, high-fat diet. (**B**) Body weight when the GTT was conducted. SD, standard diet. (**C**) Blood glucose and serum mouse C-peptide concentrations in the GTT. (**D**) Body weight, blood glucose concentrations, and tissue weights of epididymal fat, liver, and muscle at the end of the experiment. $^{**}P < 0.01$ and $^{*}P < 0.05$ versus high-fat diet/PBS group. $n = 8$.

and, thus, only transient pattern of response. This discrepancy is significant in the context of improving QOL of the patients because the latter approach would require more frequent dosing, typically several times daily, as is the case for the current open-loop therapy. Owing to its clinically acceptable durability and biosafety, our system, however, can remain effective and stable for potentially as long as 3 weeks or so depending on the volume of the reservoir.

The chemical structure of the gel described here is identical to one of those we have previously reported, which had been fine-tuned to be glucose-sensitive under physiological pH and temperature (that is, pH 7.4 and 37°C) while also revealing a gated response at around normoglycemic level of glucose (see figs. S1 and S2). In the course of fine-tuning, the focus was placed on control of the apparent pK_a (acidity) of PBA. To make the situation somewhat complicated, the pK_a depends not only on the chemical structure of PBA and other structural factors (hydrophilicity, rigidity of the main chain components, the amount of PBA, etc.) but also on the state of hydration, which is a function of a variety of environmental factors including temperature, ionic strength, pH, and sugar concentration (*17*, *18*, *20*, *21*). Meanwhile, the gated manner or "all-or-none"–type response of the gel (demonstrated in Figs. 2B and 4B) suggests how the resulting mode of insulin pharmacokinetics might be distinct in its mode of action from those resulting from linearly glucose-dependent systems, such as most closed-loop insulin delivery systems currently in use. Regarding this issue, besides its "scalability" or effectiveness at different magnitudes of release, our system also has control over the threshold value of glucose concentration at which the insulin release is commenced, based on the above-mentioned chemistry. Therefore, if necessary, one can chemically tailor the device with graded performance to treat different types of patients. The sensitivity of the gel to small physiological fluctuations in both pH (that is, acidosis or alkalosis) and temperature may be a potential concern. Regarding this matter, we have separately reported a comparative structure-function study for different gel formulations to markedly mitigate this influence (*26*).

Owing to the diffusion-dependent principle, the rate of insulin release is readily scalable, showing a linear correlation with gel surface area, assuming a constant concentration gradient of insulin across the interface over time through stable supply from the upstream reservoir. This feature provides ease-of-dose planning in a quantitative fashion, as systemically demonstrated in this study. The inherent physicochemical properties of the gel itself are also scalable. That is to say, according to the polymer free volume theory, under the premise of constant polymer chain mobility and the polymer-solute interaction, the diffusion coefficient of solutes (that is, insulin) in hydrogels is a function of the size of the solutes relative to that of the polymer chain openings or "mesh size" (*27*–*29*). As a consequence, the apparent diffusion coefficient of the solutes (insulin) in hydrogels decreases exponentially as the cross-linking density increases and as the swelling degree of the gel (the volume fraction of water within the gel) decreases. This relationship (accounted for by the polymer free volume theory) underlies quantitative basis for the skin layer–driven diffusion control accompanied by an exceptionally sharp (all-or-none type) on-off switching capability described here. Advantageously, both of these parameters, that is, cross-linking density and the swelling degree of the gel, are controllable simply on the basis of the composition of monomers and cross-linkers in feed

(in the pre-gel solution) (*17*, *18*, *20*, *21*), providing an even wider window for the scalability and optimization of the performance. The structure of the surface-coating poly(ethyleneglycol) thin layer (gel), which was intended to prevent biofouling by proteins, lipids, and other biomolecules after subcutaneous implantation, has also been carefully optimized on the basis of the above theory (*30*, *31*). Namely, this gel layer has been prepared by reaction between two four-arm branched (tetra) types of building-block macromers with controlled chain length [2500 in molecular weight (M_w) of each chain] and the end (each reactive) functional groups, resulting in the mesh size of about 10,000 with narrow distribution in terms of the molecular cutoff property, which is thus suitable for free permeation of insulin (M_w, 5807) and blockade of any larger proteins.

Our device excludes all electronics that are of absolute necessity for the current closed-loop artificial pancreas, that is, sensors, buttery, motors, microcomputers, algorithm, and electrical or wireless communication modules. In other words, all these functions have been molecularly programmed in our smart gel. The gel itself is composed of inexpensive acrylamide derivatives that are stable against heat, solvents, and even autoclave treatments. Note that all these harsh treatments easily denature any proteins that may be present, and thus are not applicable to those existing approaches using GOD and Con A. The pre-gel solution, which instantly and irreversibly gels upon heating, can fill virtually any desired shape and dimension, compatible with other existing medical device structures such as needles and catheters (as demonstrated in this study). The gel can also be combined with semipermeable type of polymeric supports such as those shaped in microneedles in either layered or interpenetrated fashions. For human use, combination with microneedle structures, among other possibilities, may provide an attractive solution to problems of scalability (owing to the large surface area of the microneedles), esthetic considerations, and the need to minimize invasiveness (*11*); in this manner, the scale discrepancy between mice and humans, which is roughly three orders of magnitude difference in weight, may be addressed theoretically. The thoroughly solution-processable fabrication, along with its heat and solvent stability, may also offer compatibility with 3D printable macro- and nanofabrication technologies. These features should offer striking advantages over the current electronics- or protein-based approaches in terms of cost, stability, and ease of mass production, transport, storage, and maintenance.

From the viewpoint of clinical translation, it is important to address how our device responds to the fluctuation of blood glucose levels under physiological and diabetic conditions in vivo. Theoretically, insulin release from the device includes the glucose-independent baseline release and the glucose-responsive inducible one. In contrast to in vitro experiments, in which the maximum insulin release rate under high-glucose conditions (200 mg/dl or higher) is at least two orders of magnitude greater than the basal insulin release rate under normoglycemic (100 mg/dl) conditions, it is technically difficult to examine these pharmacokinetic data in vivo. Nevertheless, our data show a transient and sufficient increase in serum (device-derived) human insulin concentrations. Therefore, it is likely that our device appropriately responds to the acute hyperglycemia in the glucose tolerance test and then leads to faster recovery of the blood glucose levels. On the other hand, the baseline release of human insulin from the device suppresses endogenous insulin release under several experimental conditions, which may be helpful for protection against pancreatic β cell exhaustion in type 2 diabetic patients. The next step, scaling up the protocols from mice to humans, will require tuning the chemical composition of the gel to optimize the baseline/inducible release rate for human conditions.

Currently, more than 80% of the expenditure for medical care of diabetes is made in developed countries (*1*). However, in developing countries where 80% of people with diabetes will soon live, not enough funds are spent to provide even the least expensive life-saving treatments, largely due to limited access to an adequate health care infrastructure (*2*, *32*). In this regard, the electronics-free feature of our device could potentially aid in the design of more user-friendly technology, which may facilitate its widespread use not only in developing countries but also by those patients who otherwise may not be strongly motivated, such as the elderly, infants, patients in need of nursing care, patients averse to electrical and mechanical medical devices, and so on. Further studies are required to apply our "smart gel" technology to clinical practice, such as production of the device for clinical use, confirmation of biocompatibility, and precise analysis of insulin pharmacokinetics. Nevertheless, a new paradigm aiming to develop inexpensive (disposable), more robust (tolerant of unconditioned environment), easy-to-access and easy-to-spread (even to developing regions) type of technology may eventually better address the well-recognized unmet medical needs in diabetes, that is, long-term glycemic management, avoidance of hypoglycemia, and improvement of patients' QOL.

MATERIALS AND METHODS

Reagents

N-isopropylmethacrylamide (NIPMAAm), 4-(2-acrylamidoethylcarbamoyl)-3-fluorophenylboronic acid (AmECFPBA), *N*,*N*′-methylenebisacrylamide (MBAAm), 2,2′-azobisisobutyronitrile (AIBN), FITC-labeled bovine insulin, and all organic solvents (acetone, dichloromethane, ethanol, hexane, toluene, and DMSO) were all purchased from Wako Pure Chemical Industries. NIPMAAm was recrystallized in hexane and then dried in vacuo overnight before use. Antibodies CD45-PE/Cy7, CD11b-FITC, B220-APC, CD3ε-PE, and Ly6G-APC/Cy7 for flow cytometry were purchased from BioLegend. All other reagents were purchased from Sigma-Aldrich or Nacalai Tesque and used as received, unless otherwise noted.

Preparation of gels

A slab gel shown in Fig. 2A was prepared by radical copolymerization under argon atmosphere using AIBN as an initiator in the presence of MBAAm as a cross-linking agent in DMSO. The concentrations of total monomers, AIBN, and MBAAm in feed were 3 M, 7.5 mM, and 150 mM, respectively. The composition of each monomer relative to MBAAm in feed was identical to what is indicated in Fig. 1B. The pre-gel solution was injected between two Teflon sheets (5 × 5 cm) separated by a Teflon gasket (3 mm in thickness) and backed by glass plates. The solution was polymerized at 60°C for 16 hours. The resulting gel slab was immersed successively into a series of DMSO/water mixtures graded in the order of 100/0, 75/25, 50/50, 25/75, and 0/100 to remove unreacted compounds. The slab was kept at least 1 day in each mixed solution. Cylindrically shaped "capillary" gels used for the study depicted in Fig. 2 (B and C) were prepared in an identical manner to the above, except that it was polymerized in a 1-mm-diameter glass capillary (200-μl calibrated pipets; Drummond Scientific Company).

Preparation of catheter-combined device

Silicone catheters (4 French; 1.2 mm of diameter) (Access Technologies) bearing 12 penetrating pores perpendicular to the long axis at 90° differentiated two positions (thus resulting in 48 pores on the surface) were prepared by a laser processing instrument (VLS3.50, Universal Laser

Systems). The diameter of the pore and the pitch was approximately 250 μm and 1 mm, respectively. The obtained porous catheter was washed with hot water containing detergent, steam-cleaned (Steam Cleaner SI-III, GC Corp.), sonicated in water for 10 min, and finally dried. At this stage, the first quality check in term of the resulting pore formability was made. Before gelation, the catheter surface was treated with silane coupling agent bearing methacrylate functionality [3-(trimethoxysilyl)propyl methacrylate, Shin-Etsu Chemical Co. Ltd.] to warrant the stability in the following gel attachment. Namely, the dried catheter was first plasma-cleaned in a plasma reactor (Plasma Dry Cleaner PD C210, Yamato Scientific Co. Ltd.) for 60 s with the power of 300 W under flows (15 ml/min) of oxygen and argon, exposed to the coupling reagent in 10% toluene solution for 30 min, rinsed with toluene and dichloromethane, and then incubated at 120°C for 2 hours to allow the surface silane coupling reaction. For the molded gelation (Fig. 3), an aluminum wire of 300 μl in diameter was aligned through the long axis of the catheter. This was placed in a glass capillary bearing a slightly larger inner diameter than that of the catheter, which was then filled with (the above-described) pre-gel solution. After the gelation, the gel-modified catheter containing the aluminum wire was taken out of the glass capillary and immersed in 2 M HCl aqueous solution for 1 to 2 hours until the wire becomes somewhat eroded, thus allowing for the ease of removal. The resulting gel-molded catheter was then washed with excess amount of water for 2 days and dried. At this stage, the second quality check was made in terms of the molding quality of the gel. The gel-molded catheter (cut into pieces of 15-mm length) was then connected with another longer (11 cm) piece of nontreated catheter (Fig. 3F); the thus-installed long-tail part served as an insulin reservoir. The connecting catheter had been sonicated in ethanol and plasma-cleaned before use. The connection was made by two steps: first, using heat-shrinkable tubing (SUMITUBE K, Sumitomo Electric Industries Ltd.), followed by the waterproofing treatment by use of epoxy resin [Shin-Etsu Silicone one-component RTV (KE-3424-G), Shin-Etsu Chemical Co. Ltd.]. The thus-obtained reservoir-installed device was dried at room temperature for overnight. The porous surface area of the device was further coated with a thin layer of poly(ethyleneglycol) (Tetragel) as follows. Two types of four-arm branched (tetra) poly(ethyleneglycol) macromers of 10,000 in M_w (2500 for each chain) bearing either amino (100PA, NOF Corp.) or active ester (*N*-hydroxysuccinimide–activated) groups at each four end (100CS, NOF Corp.) were dissolved separately in PBS (1 g/20 ml) adjusted to be pH 7.4 and pH 5.8, respectively. These were mixed in a stoichiometric ratio and quickly homogenized at room temperature, to which the device was gently immersed and then kept overnight under high-humidity atmosphere. Thereafter, the device was autoclaved (121°C for 25 min) and dried. Before insulin load, the most frontal (gel-modified) part of the device was immersed in PBS and kept overnight at room temperature under sterilized conditions. Finally, the device was filled with recombinant human insulin (Humulin R, Eli Lilly Japan K.K.) and used for the animal study.

Imaging of the device

In the course of preparation and in vivo study, cross sections of the device were examined by digital optical microscopy and scanning electron microscopy (SEM). Devices immersed in optimum cutting temperature (OCT) compound (OCT Compound 4583, VWR International LLC) were placed vertically in cryomold [Tissue-Tek Cryomold Biopsy (15 × 15 × 5 mm), VWR International LLC]. Then, the suspensions in cryomold were placed on a freezing microtome sample holder (Leica CM1950, Leica Biosystems Inc.) for freezing. Obtained frozen suspensions were sectioned with a thickness of 50 μm using a freezing microtome (Leica CM1950) and then washed three times with Milli-Q water to remove the OCT compound. After washing, the sections were analyzed on a digital microscope (RH 2000 coupled with MXB-2016Z, Hirox Co. Ltd.) (fig. S3). Thereafter, the sections were transferred onto a carbon tape and dried overnight at room temperature. Morphologies of the dried sections were visualized by a benchtop SEM system (JCM-6000, JEOL Co. Ltd.) after gold coating with a sputter coater (SC-701AT047-9010 Quick Auto Coater, Sanyu Co. Ltd.) (figs. S4 to S6).

Release experiments

Release experiments were carried out using an HPLC system (JASCO) equipped with two pumps and internal detectors for refractive index (RI) and fluorescence intensities (fig. S10). Insulin was loaded into the gel (capillary gel) or catheter-combined device by immersing them in PBS containing FITC-labeled bovine insulin (130 mg/liter) at 4°C for 24 hours. The insulin-loaded gel or device was then transferred to a 0.01 M HCl aqueous solution and incubated at 37°C for 30 min to form the skin layer on its surface for the entrapment of the FITC-labeled insulin. This treatment was meant for shortening the time required for the skin layer formation (*19*). The insulin-loaded gel or device was then put in a Tricorn Empty High-Performance Column (GE Healthcare) having dimensions of 10 and 50 mm in inner diameter and length, respectively. The column was settled in a thermostated (at 37°C) flow of PBS (pH 7.4; 155 mM NaCl) containing glucose (100 mg/dl), the flow rate of which was constantly 1 ml/min in a chamber connected to the HPLC system. The initial equilibration was allowed until no leakage of insulin from the device (or gel) was observable, which typically took a few hours. The fluorescence intensity of the solution at 520 nm (excitation wavelength, 495 nm) was monitored to quantify the released amount of FITC-labeled insulin from the device (or gel) based on calibration. Two solutions, PBS with and without glucose (1000 mg/dl), were prepared and supplied through the two pumps of the system. The mixing fraction of the two pump supply was continuously controlled by the equipped software (ChromNAV, JASCO) to provide desired temporal gradient patterns of the glucose concentration between 100 and 500 mg/dl. In situ glucose concentration was monitored at the chamber outflow by the RI detector throughout the experiment. The calibration was carried out by measuring standard PBS containing FITC-labeled insulin with a range of concentrations between 240 pM and 125 nM. The obtained calibration curve was fitted by the following quadratic equation: $I = 39{,}222C - 40C^2$ ($R^2 = 0.999$), where I is the observed fluorescence intensity, and C is the concentration (in nanomolars) of FITC-labeled insulin. This equation was used to assess the discrepancy in the rate of insulin release under two distinct equilibrium states, that is, hyperglycemic (200 mg/dl) and normoglycemic (100 mg/dl) conditions. For a single device, the former was calculated to be on the order of 10 to 100 nM, whereas the latter was found to be below the detection limit, which is less than 100 pM.

Animals

Eight-week-old C57BL/6J mice were purchased from CLEA Japan. They were maintained in a temperature-, humidity-, and light-controlled room (12-hour light/dark cycles) and allowed free access to water and standard chow (343.1 kcal/100 g, 12.6% energy as fat; CE-2, CLEA Japan). Type 1 diabetic mice were generated by intraperitoneal injection of STZ (125 mg/kg body weight for 3 consecutive days). Type 2 diabetic mice were generated by feeding of high-fat diet (556 kcal/100 g, 60% energy as fat; D12492, Research Diets) for 4 weeks. The catheter-combined

device containing 150 μl of recombinant human insulin or PBS was implanted subcutaneously in the back skin of the mice. All in vivo experiments in this study were approved by the Animal Care and Use Committee of Nagoya University (approval number 16072).

Cell culture

3T3-L1 preadipocytes were purchased from American Type Culture Collection. Differentiation of 3T3-L1 preadipocytes to adipocytes was described elsewhere (*33*). Cells at day 10 after the induction of differentiation were used for the insulin-dependent glucose uptake experiments. After the change of culture medium containing different amounts of glucose (that is, 450 and 100 mg/dl), the gel pieces were put on the Transwell inserts with a 0.4-μm porous membrane (Corning), and the change of each medium glucose concentration was monitored.

Glucose, fructose, and aspartame tolerance test

The glucose tolerance test was performed as described (*34*). Briefly, blood glucose concentrations were measured at 0, 15, 30, 60, 90, and 120 min after intraperitoneal injection of glucose (1 to 3 g/kg body weight) by a blood glucose test meter (Glutest Mint, Sanwa-Kagaku). The fructose (2 g/kg body weight) and aspartame (0.1 g/kg body weight) tolerance tests were performed similarly to the glucose tolerance test.

Blood analysis

Serum human and mouse insulin and mouse C-peptide concentrations were measured using commercially available enzyme-linked immunosorbent assay kits (human insulin, Mercodia AB; mouse insulin and mouse C-peptide, Morinaga). HbA1c was measured using Quo-Lab (Nipro). Flow cytometry analysis was performed to evaluate the populations of white blood cells using the MACSQuant Analyzer 10 (Miltenyi Biotec) and FlowJo 9.7.7 software (Tomy Digital Biology). T cells, B cells, neutrophils, and monocytes were identified by $CD3\varepsilon^+$, $B220^+$, $CD11b^+Ly6G^+$, and $CD11b^+Ly6G^-$ in $CD45^+$ cells, respectively.

Quantitative real-time polymerase chain reaction

Total RNA was extracted from the liver, and quantitative real-time polymerase chain reaction (PCR) was performed as described (*34*). Briefly, 10 ng of complementary DNA was used for real-time PCR amplification with SYBR Green Detection Protocol using StepOnePlus (Life Technologies). Primers used in this study were as follows: C-X-C chemokine receptor type 2 (CXCR2) sense, 5′-GGTGACTCTGCTGAGCCTTGT-3′; CXCR2 antisense, 5′-GCAGGTGCTCCGGTTGTATAA-3′; G6Pase sense, 5′-CACCTGTGAGACCGGACCA-3′; G6Pase antisense, 5′-GACCATAACATAGTATACACCTGCTGC-3′; interleukin-6 (IL-6) sense, 5′-CCAGAGATACAAAGAAATGATGG-3′; IL-6 antisense, 5′-ACTCCAGAAGACCAGAGGAAAT-3′; monocyte chemoattractant protein-1 (MCP-1) sense, 5′-CCACTCACCTGCTGCTACTCAT-3′; MCP-1 antisense, 5′-TGGTGATCCTCTTGTAGCTCTCC-3′; PEPCK sense, 5′-CCACAGCTGCTGCAGAACA-3′; PEPCK antisense, 5′-GAAGGGTCGCATGGCAAA-3′. The F4/80, FAS, SREBP-1c, TNFα (tumor necrosis factor–α), and 36B4 primers were described previously (*35*). Data were normalized to the 36B4 levels and analyzed using the comparative C_t (cycle threshold) method.

Colony formation assay

Biosafety of the device was evaluated in vitro on the basis of *ISO 10993-1 Biological Evaluation of Medical Devices—Part 1: Evaluation and Testing within a Risk Management Process* and *ISO 10993-5 Biological Evaluation of Medical Devices—Part 5: Tests for in vitro cytotoxicity*. Chinese hamster lung fibroblasts (V79) were cultured in Eagle's minimum essential medium (MEM) supplemented with 10% fetal bovine serum (FBS). Eight pieces of catheter-combined device, polyurethane film (negative control), and polyurethane film containing 0.1% of zinc diethyldithiocarbamate (positive control) were extracted in M05 medium (Eagle's MEM supplemented with 5% FBS and 1 mM sodium pyruvate) at the concentration of 0.1 g/ml. After incubation in a 5% CO_2 incubator at 37°C for 24 hours, the conditioned media were designated to be 100% extract. The 100% extract was diluted with M05 medium, and these were added to prepared V79 cells. After 6 days, the cells were fixed with methanol and stained by 10% Giemsa staining solution. The number of colonies on each well was counted, and relative plating efficiency was calculated as a ratio of the number of colonies in the sample to that in the control.

Histological analysis

The skin with control silicone catheter or the catheter-combined device was fixed with neutral-buffered formalin and embedded in paraffin. Sections (2 mm thick) were stained with hematoxylin and eosin and Masson's trichrome.

Statistical analysis

Data are means ± SEM, and $P < 0.05$ and $P < 0.01$ were considered statistically significant. Statistical analysis was performed using analysis of variance (ANOVA), followed by Tukey-Kramer test. Unpaired *t* test was used to compare two groups.

SUPPLEMENTARY MATERIALS

Supplementary material for this article is available at http://advances.sciencemag.org/cgi/content/full/3/11/eaaq0723/DC1

fig. S1. Phase diagram of the gel.
fig. S2. Assessment of skin layer formation.
fig. S3. Optical images of the device sections.
fig. S4. SEM images of the device sections without poly(ethyleneglycol) coating.
fig. S5. SEM images of the device sections with poly(ethyleneglycol) coating.
fig. S6. SEM images of the poly(ethyleneglycol)-coated device sections after 1 week in vivo implantation.
fig. S7. Optical images of the device after 1 week in vivo implantation.
fig. S8. Investigation of biosafety of the device in vitro and in vivo.
fig. S9. Evaluation of long-term efficacy of the device in vivo.
fig. S10. Diagram of the HPLC setup used for release experiments.

REFERENCES AND NOTES

1. W. T. Cefalu, J. B. Buse, J. Tuomilehto, G. A. Fleming, E. Ferrannini, H. C. Gerstein, P. H. Bennett, A. Ramachandran, I. Raz, J. Rosenstock, S. E. Kahn, Update and next steps for real-world translation of interventions for type 2 diabetes prevention: Reflections from a Diabetes Care Editors' expert forum. *Diabetes Care* **39**, 1186–1201 (2016).
2. E. Ginter, V. Simko, Type 2 diabetes mellitus, pandemic in 21st century. *Adv. Exp. Med. Biol.* **771**, 42–50 (2013).
3. A. N. Zaykov, J. P. Mayer, R. D. DiMarchi, Pursuit of a perfect insulin. *Nat. Rev. Drug Discov.* **15**, 425–439 (2016).
4. Y. Ohkubo, H. Kishikawa, E. Araki, T. Miyata, S. Isami, S. Motoyoshi, Y. Kojima, N. Furuyoshi, M. Shichiri, Intensive insulin therapy prevents the progression of diabetic microvascular complications in Japanese patients with non-insulin-dependent diabetes mellitus: A randomized prospective 6-year study. *Diabetes Res. Clin. Pract.* **28**, 103–117 (1995).
5. Diabetes Control and Complications Trial Research Group, The effect of intensive treatment of diabetes on the development and progression of long-term complications in insulin-dependent diabetes mellitus. *N. Engl. J. Med.* **329**, 977–986 (1993).
6. M. Shichiri, H. Kishikawa, Y. Ohkubo, N. Wake, Long-term results of the Kumamoto Study on optimal diabetes control in type 2 diabetic patients. *Diabetes Care* **23**, B21–B29 (2000).
7. K. Kumareswaran, M. L. Evans, R. Hovorka, Closed-loop insulin delivery: Towards improved diabetes care. *Discov. Med.* **13**, 159–170 (2012).

8. R. Hovorka, Continuous glucose monitoring and closed-loop systems. *Diabet. Med.* **23**, 1–12 (2006).
9. Y. Qiu, K. Park, Environment-sensitive hydrogels for drug delivery. *Adv. Drug Deliv. Rev.* **53**, 321–339 (2001).
10. T. Miyata, T. Uragami, K. Nakamae, Biomolecule-sensitive hydrogels. *Adv. Drug Deliv. Rev.* **54**, 79–98 (2002).
11. J. C. Yu, Y. Zhang, Y. Ye, R. DiSanto, W. Sun, D. Ranson, F. S. Ligler, J. B. Buse, Z. Gu, Microneedle-array patches loaded with hypoxia-sensitive vesicles provide fast glucose-responsive insulin delivery. *Proc. Natl. Acad. Sci. U.S.A.* **112**, 8260–8265 (2015).
12. O. Veiseh, B. C. Tang, K. A. Whitehead, D. G. Anderson, R. Langer, Managing diabetes with nanomedicine: Challenges and opportunities. *Nat. Rev. Drug Discov.* **14**, 45–57 (2015).
13. T. G. Farmer Jr., T. F. Edgar, N. A. Peppas, The future of open- and closed-loop insulin delivery systems. *J. Pharm. Pharmacol.* **60**, 1–13 (2008).
14. X. Chen, J. Luo, W. Wu, H. Tan, F. Xu, J. Li, The influence of arrangement sequence on the glucose-responsive controlled release profiles of insulin-incorporated LbL films. *Acta Biomater.* **8**, 4380–4388 (2012).
15. J. Luo, S. Cao, X. Chen, S. Liu, H. Tan, W. Wu, J. Li, Super long-term glycemic control in diabetic rats by glucose-sensitive LbL films constructed of supramolecular insulin assembly. *Biomaterials* **33**, 8733–8742 (2012).
16. K. Kataoka, H. Miyazaki, M. Bunya, T. Okano, Y. Sakurai, Totally synthetic polymer gels responding to external glucose concentration: Their preparation and application to on-off regulation of insulin release. *J. Am. Chem. Soc.* **120**, 12694 (1998).
17. A. Matsumoto, S. Ikeda, A. Harada, K. Kataoka, Glucose-responsive polymer bearing a novel phenylborate derivative as a glucose-sensing moiety operating at physiological pH conditions. *Biomacromolecules* **4**, 1410–1416 (2003).
18. A. Matsumoto, T. Ishii, J. Nishida, H. Matsumoto, K. Kataoka, Y. Miyahara, A synthetic approach toward a self-regulated insulin delivery system. *Angew. Chem. Int. Ed. Engl.* **51**, 2124–2128 (2012).
19. A. Matsumoto, T. Kurata, D. Shiino, K. Kataoka, Swelling and shrinking kinetics of totally synthetic, glucose-responsive polymer gel bearing phenylborate derivative as a glucose-sensing moiety. *Macromolecules* **37**, 1502–1510 (2004).
20. A. Matsumoto, K. Yamamoto, R. Yoshida, K. Kataoka, T. Aoyagi, Y. Miyahara, A totally synthetic glucose responsive gel operating in physiological aqueous conditions. *Chem. Commun.* **46**, 2203–2205 (2010).
21. A. Matsumoto, R. Yoshida, K. Kataoka, Glucose-responsive polymer gel bearing phenylborate derivative as a glucose-sensing moiety operating at the physiological pH. *Biomacromolecules* **5**, 1038–1045 (2004).
22. E. Galbraith, T. D. James, Boron based anion receptors as sensors. *Chem. Soc. Rev.* **39**, 3831–3842 (2010).
23. A. R. Martin, J.-J. Vasseur, M. Smietana, Boron and nucleic acid chemistries: Merging the best of both worlds. *Chem. Soc. Rev.* **42**, 5684–5713 (2013).
24. A. Matsumoto, K. Kataoka, Y. Miyahara, New directions in the design of phenylboronate-functionalized polymers for diagnostic and therapeutic applications. *Polym. J.* **46**, 483–491 (2014).
25. D. H.-C. Chou, M. J. Webber, B. C. Tang, A. B. Lin, L. S. Thapa, D. Deng, J. V. Truong, A. B. Cortinas, R. Langer, D. G. Anderson, Glucose-responsive insulin activity by covalent modification with aliphatic phenylboronic acid conjugates. *Proc. Natl. Acad. Sci. U.S.A.* **112**, 2401–2406 (2015).
26. A. Matsumoto, Y. Mai, M. Hiroko, S. Mai, T. Miyuki, G. Tatsuro, H. Toru, A. Takao, M. Yuji, Boronate-functionalized polymer gel-based insulin delivery system with improved stability in performance: A comparative structure-function study. *Chem. Lett.* **45**, 460–462 (2016).
27. J. S. Vrentas, J. L. Duda, Diffusion in polymer-solvent systems. II. A predictive theory for dependence of diffusion-coefficients on temperature, concentration, and molecular weight. *J. Polym. Sci. B Polym. Phys.* **15**, 417–439 (1977).
28. P. G. De Gennes, Dynamics of entangled polymer solutions. I. The Rouse model. *Macromolecules* **9**, 587–593 (1976).
29. S. Matsukawa, I. Ando, A study of self-diffusion of molecules in polymer gel by pulsed-gradient spin-echo ^{1}H NMR. *Macromolecules* **29**, 7136–7140 (1996).
30. T. Sakai, T. Matsunaga, Y. Yamamoto, C. Ito, R. Yoshida, S. Suzuki, N. Sasaki, M. Shibayama, U.-i. Chung, Design and fabrication of a high-strength hydrogel with ideally homogeneous network structure from tetrahedron-like macromonomers. *Macromolecules* **41**, 5379–5384 (2008).
31. T. Sakai, Gelation mechanism and mechanical properties of Tetra-PEG gel. *React. Funct. Polym.* **73**, 898–903 (2013).
32. General Assembly resolution 61/225, World Diabetes Day, 14 November 2006; www.worlddiabetesday.org.
33. T. Suganami, J. Nishida, Y. Ogawa, A paracrine loop between adipocytes and macrophages aggravates inflammatory changes: Role of free fatty acids and tumor necrosis factor α. *Arterioscler. Thromb. Vasc. Biol.* **25**, 2062–2068 (2005).
34. M. Tanaka, K. Ikeda, T. Suganami, C. Komiya, K. Ochi, I. Shirakawa, M. Hamaguchi, S. Nishimura, I. Manabe, T. Matsuda, K. Kimura, H. Inoue, Y. Inagaki, S. Aoe, S. Yamasaki, Y. Ogawa, Macrophage-inducible C-type lectin underlies obesity-induced adipose tissue fibrosis. *Nat. Commun.* **5**, 4982 (2014).
35. M. Itoh, T. Suganami, N. Nakagawa, M. Tanaka, Y. Yamamoto, Y. Kamei, S. Terai, I. Sakaida, Y. Ogawa, Melanocortin 4 receptor–deficient mice as a novel mouse model of nonalcoholic steatohepatitis. *Am. J. Pathol.* **179**, 2454–2463 (2011).

Acknowledgments: We thank R. Miyake (University of Tokyo) for technical advice in microprocessing of catheter. **Funding:** This work was supported in part by grants-in-aid for scientific research from the Ministry of Education, Culture, Sports, Science and Technology of Japan (MEXT), the Cooperative Research Project of Research Center for Biomedical Engineering (MEXT), Japan Science and Technology Agency (Start-ups from Advanced Research and Technology program and Center of Innovation stream), and Japan Agency for Medical Research and Development (Acceleration Transformative Research for Medical Innovation program). This work was also supported by research grants from the Canon Foundation, the Secom Science and Technology Foundation, the Terumo Foundation for Life Sciences and Arts, the Mochida Memorial Foundation for Medical and Pharmaceutical Research, and Kanagawa Institute of Industrial Science and Technology.
Author contributions: A.M., M.T., H.M., K.O., Y.M.-o., H.K., H.Y., I.S., and T.M. performed most of the experiments and analyzed the data. H.I., K.K., Y.O., and Y.M. contributed to the design and interpretation of the study. A.M. and T.S. conceived and coordinated the research, contributed to the discussion, and wrote the manuscript. All authors reviewed the manuscript. **Competing interests:** A.M., K.K., and Y.M. are inventors on two patents related to this work filed by the National Institute for Materials Science (PCT/JP2010/073544, filed on 27 December 2010 and published on 13 July 2016; and PCT/JP2011/061869, filed on 24 May 2011 and published on 12 July 2017). A.M., H.M., T.S., M.T., and Y.M. are inventors on a patent application related to this work filed by the Tokyo Medical and Dental University (PCT/JP2016/081407, filed on 24 October 2016). All other authors declare that they have no competing interests. **Data and materials availability:** All data needed to evaluate the conclusions in the paper are present in the paper. Additional data related to this paper may be requested from the authors.

Submitted 27 September 2017
Accepted 27 October 2017
Published 22 November 2017
10.1126/sciadv.aaq0723

Citation: A. Matsumoto, M. Tanaka, H. Matsumoto, K. Ochi, Y. Moro-oka, H. Kuwata, H. Yamada, I. Shirakawa, T. Miyazawa, H. Ishii, K. Kataoka, Y. Ogawa, Y. Miyahara, T. Suganami, Synthetic "smart gel" provides glucose-responsive insulin delivery in diabetic mice. *Sci. Adv.* **3**, eaaq0723 (2017).